JOURNAL OF PROPULSION AND POWER
Vol. 17, No. 2, March–April 2001

Advanced Sub-Model for Airblast Atomizers

Y. Liao,* S. M. Jeng,† and M. A. Jog‡
University of Cincinnati, Cincinnati, Ohio 45221
and
M. A. Benjamin§
Parker Hannifin Corporation, Mentor, Ohio 44060

A three-dimensional viscous stability analysis has been carried out to model airblast atomization. The model considers an annular liquid sheet downstream of an airblast atomizer and incorporates essential features, such as three-dimensional disturbances, liquid viscosity, inner and outer air swirl, and finite film thickness. Effects of axial velocity, air swirl, and liquid viscosity on the growth rates of various disturbance modes have been examined in detail. It has been found that increasing the relative axial velocity between the liquid and the gas phases significantly improves the fuel atomization. The inner and outer air moving together enhances the instability of the liquid sheet more significantly than only the inner or outer air. When air swirl is absent, the axisymmetric mode dominates the breakup process of the liquid sheet. Liquid viscosity is found to have a twofold effect: reduce the growth rates of unstable waves and shift the dispersion diagram toward long waves. Air swirl not only promotes the instability of the liquid sheet, but also switches the dominant mode from the axisymmetric mode to a helical mode. A combination of the inner and outer air swirl improves airblast atomization more significantly than a single air swirl.

Nomenclature

A	=	vortex strength, m^2/s
c	=	wave propagation speed, m/s
f	=	frequency, Hz
h	=	ratio of inner to outer radius, R_a/R_b
I_n	=	nth-order modified Bessel function of the first kind
K_n	=	nth-order modified Bessel function of the second kind
k	=	axial wave number, $2\pi f/c$, 1/m
n	=	azimuthal wave number
P	=	mean pressure, N/m^2
p	=	disturbance pressure, N/m^2
R_a	=	inner radius of liquid sheet, m
R_b	=	outer radius of liquid sheet, m
Re	=	Reynolds number, $\rho_l U_l R_b/\mu$
r	=	radial coordinate, m
t	=	time, s
U	=	mean axial velocity, m/s
u	=	disturbance axial velocity, m/s
V	=	mean radial velocity, m/s
v	=	disturbance radial velocity, m/s
W	=	mean tangential velocity, m/s
We	=	Weber number, $\rho U^2 R_b/\sigma$
w	=	disturbance tangential velocity, m/s
x	=	axial coordinate, m
η	=	displacement disturbance, m
θ	=	azimuthal angle, rad
μ	=	fluid viscosity, N s/m^2
ρ	=	fluid density, kg/m^3
σ	=	surface tension kg/s^2
Ω	=	angular velocity, 1/s
ω	=	temporal frequency, 1/s

Subscripts

i	=	inner gas
l	=	liquid phase
o	=	outer gas
si	=	based on inner air swirling component
so	=	based on outer air swirling component

Presented as Paper 99-2207 at the AIAA/ASME/SAE/ASEE 35th Joint Propulsion Conference and Exhibit, Los Angeles, CA, 20–24 June 1999; received 24 November 1999; accepted for publication 13 April 2000.

*Research Assistant Professor, Department of Aerospace Engineering and Engineering Mechanics.
†Professor, Department of Aerospace Engineering and Engineering Mechanics. Member AIAA.
‡Associate Professor, Department of Mechanical, Industrial and Nuclear Engineering.
§Technical Team Leader, Gas Turbine Fuel Systems Division. Member AIAA.

I. Introduction

MEETING emission requirements and constantly improving combustion efficiency remain to be two primary challenges for the development of next generation gas turbine engines. For example, to lower emission level of NO_x significantly, it is crucial to optimize the fuel atomization process and combustor aerodynamics to achieve rapid and uniform fuel/air mixing. Because of its desirable attributes, such as lower fuel pressure requirement, larger flow turn-down ratio, and lower pollutant emissions, the airblast atomizer has been considered as an advanced fuel injection device and is widely used in gas turbine engines and oil-fired furnaces. In an airblast atomizer, kinetic energy of the high-speed swirling airstreams is used to breakup the liquid sheet. According to the filming method, airblast atomizers can be divided into two types, namely, prefilming airblast atomizer and swirl-cup airblast atomizer. Inside a traditional prefilming airblast atomizer,[1] liquid fuel first spreads out into a thin annular sheet and then is exposed to high-speed swirling airstreams on both sides, as shown in Fig. 1. In the modern swirl-cup airblast atomizer, liquid fuel emanates from a pressure-swirl atomizer in the form of a conical liquid sheet and impinges with the swirler cup forming an annular liquid film. This thin liquid film is driven by fast moving inner air to the nozzle tip, and atomization occurs as a result of the strong shear action of the inner and outer airstreams. Therefore, for both types of airblast atomizers, the annular liquid sheet is subjected to swirling airstreams and its breakup is responsible for spray formation and determines the resultant spray characteristics such as mean droplet diameter and droplet size distribution. The subsequent combustion process in a gas turbine engine is significantly affected by the initial droplet distribution. Therefore, understanding the underlying mechanisms that govern fuel atomization in airblast atomizers is critically important in developing next generation gas turbine engines. A stability model that identifies specific effects of various forces on the breakup process of the liquid sheet is useful in improving atomizer design. Also, computational simulations of spray combustion in gas turbine engines use droplet

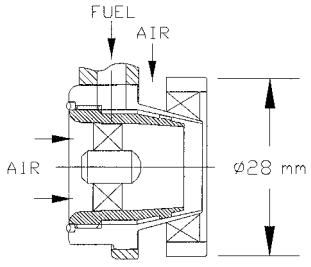

Fig. 1 Schematic of a prefilming airblast atomizer.

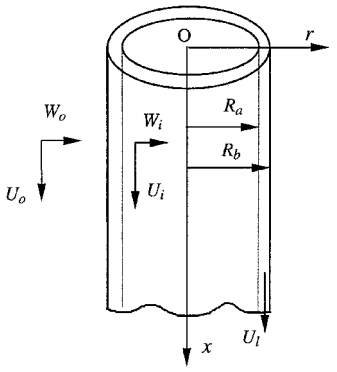

Fig. 2 Annular liquid sheet subjected to swirling airstreams.

distribution in a spray emanating from a fuel atomizer as initial conditions. The success of such simulations in part depends on the accuracy of the droplet size distribution used. Therefore, establishment of an advanced stability model will also benefit the computational fluid dynamics design/simulation tools for gas turbine engines.[2]

It is well established that the disintegration of a liquid sheet is due to the growth of unstable waves at the liquid/gas interface. The growth rates of these unstable waves depends on flow conditions, fluid properties, nozzle geometry, and boundary conditions. Extensive theoretical and experimental studies have demonstrated that, among unstable waves, there exists a wave number k or frequency $f = kc/2\pi$ that has the maximum growth rate. This wave is called the most unstable wave and dominates the breakup of the liquid sheet. Its wavelength is related to the mean droplet size, and its growth rate determines the breakup length. Stability analysis to predict the most unstable wave number and the maximum growth rate in atomization of planar liquid sheets has received much attention in the literature.[3–9] More recently, recognizing the potential of airblast atomizer in meeting more stringent emission requirements, existing stability models for planar (two-dimensional) sheets have been extended to annular liquid sheets.[10–16] Theoretical models for the instability of annular liquid sheets have been summarized in a recent paper.[16] In that paper, we considered effects of inner as well as outer air swirl. It was found that increasing the relative velocity between the liquid and gas phases increases both the most unstable wave number and the maximum growth rate. As a result, atomization quality is significantly improved. It was also found that air swirl destabilizes the annular liquid sheet. These conclusions have been validated by several experimental investigations[17–19] that revealed that the swirling airstream promotes the disintegration of the liquid sheet, apart from enhancing fuel/air mixing and stabilizing the flame.

However, our previous model[16] neglected the effect of liquid viscosity. Dombrowski and Johns[6] have shown that liquid viscosity has a significant effect on the size of droplets formed from breakup of planar liquid sheets. However, for annular liquid sheets, a stability model that considers liquid viscosity is not available in literature. Such a model is developed in the present paper. Here, we extend the inviscid analysis by considering liquid viscosity while maintaining essential features such as three-dimensional disturbances, inner and outer air swirl, and an annular geometry with finite film thickness. The most unstable wave number and the maximum growth rate are predicted. Effects of liquid viscosity on the growth rates of the axisymmetric and various helical modes have been examined under both nonswirling and swirling flow conditions. Effects of air swirl on the growth rates of both the axisymmetric ($n = 0$) and the first two helical modes ($n = 1$ and 2) are investigated and compared. The results reported here confirm that our previous inviscid model[16] can be successfully recovered from the present model in the limit of large Reynolds number. Because the flow conditions considered in this paper are quite similar to the practical operating conditions, it is expected that the present analysis will elucidate the breakup behavior of a liquid sheet downstream of an airblast or air-assisted atomizer. Also note that other geometric conditions such as plane liquid sheet or round liquid jet can be recovered from the present model as the ratio of inner to outer radius approaches 1 or 0, respectively. As such, this three-dimensional viscous stability model sheds lights on the underlying mechanism of liquid atomization and provides guidance for the design of airblast as well as pressure atomizers.

II. Mathematical Model

The geometrical and flow conditions considered here are shown in Fig. 2. A viscous annular liquid sheet is subjected to coaxial swirling airstreams. In the stability model, the gas phase is assumed to be inviscid and incompressible. Mean flows of the liquid, the inner air, and the outer air are assumed to be $(U_l, 0, 0)$, $(U_i, 0, \Omega r)$, and $(U_o, 0, A/r)$, respectively. This combination of solid body rotation and free vortex profile is quite similar to the practical tangential velocity profile inside a gas turbine combustor. To maintain an annular shape of the liquid surface when undisturbed, a constraint on the mean pressure of the inner and outer airstreams at the interfaces must be imposed by Eq. (1):

$$P_i - P_o = \sigma(1/R_a + 1/R_b) \tag{1}$$

A. Linearized Disturbance Equations

The velocity, pressure, and displacement disturbances are assumed to have the forms

$$(u, v, w, p') = [\hat{u}(r), \hat{v}(r), \hat{w}(r), \hat{p}(r)]\exp[i(kx + n\theta - \omega t)] \tag{2}$$

$$\eta_j(x, \theta, t) = \hat{\eta}_j \exp[i(kx + n\theta - \omega t)] \qquad j = i, o \tag{3}$$

To derive the linearized disturbance equations, velocity and pressure disturbances are superposed on their mean counterparts as

$$\boldsymbol{V} = \bar{\boldsymbol{V}} + \boldsymbol{v}, \qquad p = \bar{P} + p' \tag{4}$$

where

$$\boldsymbol{V} = \begin{pmatrix} U \\ V \\ W \end{pmatrix}, \qquad \boldsymbol{v} = \begin{pmatrix} u \\ v \\ w \end{pmatrix}$$

The overbar in Eq. (4) represents the assumed mean flow quantities and the prime indicates disturbance. The linearized disturbance equations for the liquid phase can be written in vector form as

$$\nabla \cdot \boldsymbol{v} = 0 \tag{5}$$

$$\rho_l\left(\frac{\partial \boldsymbol{v}}{\partial t} + U_l\frac{\partial \boldsymbol{v}}{\partial x}\right) = -\nabla p_l' + \mu\nabla^2\boldsymbol{v} \tag{6}$$

For the inner and outer airstreams, the linearized disturbance equations are written in component form as

$$\frac{\partial u}{\partial x} + \frac{v}{r} + \frac{\partial v}{\partial r} + \frac{1}{r}\frac{\partial w}{\partial \theta} = 0 \tag{7}$$

$$\frac{\partial u}{\partial t} + \frac{W_j}{r}\frac{\partial u}{\partial \theta} + U_j\frac{\partial u}{\partial x} = -\frac{1}{\rho_j}\frac{\partial p_j'}{\partial x} \tag{8}$$

$$\frac{\partial v}{\partial t} + U_j\frac{\partial v}{\partial x} + \frac{W_j}{r}\frac{\partial v}{\partial \theta} - \frac{2W_j w}{r} = -\frac{1}{\rho_j}\frac{\partial p_j'}{\partial r} \tag{9}$$

$$\frac{\partial w}{\partial t} + v\frac{\mathrm{d}W_j}{\mathrm{d}r} + \frac{W_j}{r}\frac{\partial w}{\partial \theta} + U_j\frac{\partial w}{\partial x} + \frac{W_j v}{r} = -\frac{1}{\rho_j}\frac{\partial p_j'}{r\partial \theta} \tag{10}$$

where $j = i, o$, $W_i = \Omega r$, and $W_o = A/r$.

B. Boundary Conditions

To solve the given linearized disturbance equations, both kinematic and dynamic boundary conditions must be prescribed at the interfaces for both the liquid and gas phases. The kinematic boundary condition requires that the radial velocity component be continuous across the interfaces, that is, particles on the interface remain there. Mathematically, they are expressed as follows:

$$v = \frac{\partial \eta_i}{\partial t} + \Omega \frac{\partial \eta_i}{\partial \theta} + U_i \frac{\partial \eta_i}{\partial x} \qquad \text{at} \qquad r = R_a \tag{11}$$

$$v = \frac{\partial \eta_o}{\partial t} + \frac{A}{r^2} \frac{\partial \eta_o}{\partial \theta} + U_o \frac{\partial \eta_o}{\partial x} \qquad \text{at} \qquad r = R_b \tag{12}$$

$$v = \frac{\partial \eta_i}{\partial t} + U_l \frac{\partial \eta_i}{\partial x} \qquad \text{at} \qquad r = R_a \tag{13}$$

$$v = \frac{\partial \eta_o}{\partial t} + U_l \frac{\partial \eta_o}{\partial x} \qquad \text{at} \qquad r = R_b \tag{14}$$

The dynamic boundary conditions at the inner and outer interfaces require balance of forces including pressure force, surface tension, centrifugal force, and viscous force in the radial direction. In the axial and azimuthal direction, due to the inviscid assumption of the airstreams, viscous stress at the liquid/air interfaces are zero:

$$p_l' - p_i' = \sigma \left(\frac{\eta_i}{R_a^2} + \frac{1}{R_a^2} \frac{\partial^2 \eta_i}{\partial \theta^2} + \frac{\partial^2 \eta_i}{\partial x^2} \right) + \rho_i \Omega^2 R_a \eta_i + 2\mu \frac{\partial v}{\partial r} \qquad \text{at} \qquad r = R_a \tag{15}$$

$$p_l' - p_o' = -\sigma \left(\frac{\eta_o}{R_b^2} + \frac{1}{R_b^2} \frac{\partial^2 \eta_o}{\partial \theta^2} + \frac{\partial^2 \eta_o}{\partial x^2} \right) - \frac{\rho_o A^2 \eta_o}{R_b^3} + 2\mu \frac{\partial v}{\partial r} \qquad \text{at} \qquad r = R_b \tag{16}$$

$$\tau_{rx} = \mu \left(\frac{\partial u}{\partial r} + \frac{\partial v}{\partial x} \right) = 0 \qquad \text{at} \qquad r = R_a,\ R_b \tag{17}$$

$$\tau_{r\theta} = \mu \left(\frac{\partial w}{\partial r} - \frac{w}{r} + \frac{1}{r} \frac{\partial v}{\partial \theta} \right) = 0 \qquad \text{at} \qquad r = R_a,\ R_b \tag{18}$$

C. Nondimensional Dispersion Equation

To isolate the specific effect of flow conditions, fluid properties, and geometric parameters on the instability of the annular liquid sheet, the following nondimensional parameters are introduced:

$$We_i = \rho_i U_i^2 R_b / \sigma, \qquad We_o = \rho_o U_o^2 R_b / \sigma, \qquad We_l = \rho_l U_l^2 R_b / \sigma$$

$$We_{\mathrm{so}} = \rho_o A^2 / \sigma R_b, \qquad We_{\mathrm{si}} = \rho_i \Omega^2 R_b^3 / \sigma, \qquad Re = \rho_l U_l R_b / \mu$$

$$\bar{\rho}_i = \rho_i / \rho_l, \qquad \bar{\rho}_o = \rho_o / \rho_l, \qquad h = R_a / R_b$$

$$\bar{k} = k R_b, \qquad \bar{\omega} = \omega R_b / U_l$$

$$\bar{s} = s R_b = \sqrt{\bar{k}^2 + Re(-i\bar{\omega} + i\bar{k})}, \qquad s = \sqrt{k^2 + (-i\omega + ikU_l)/\nu} \tag{19}$$

Derivation of the nondimensional dispersion equation is very lengthy and is given in Ref. 20. The final dispersion equation can be expressed as

$$\left(l_1 \bar{\omega}^4 + l_2 \bar{\omega}^3 + l_3 \bar{\omega}^2 + l_4 \bar{\omega} + l_5\right) - \bar{\rho}_i \times (-\bar{\omega} + l_6) \times \frac{\left(l_7 \bar{\omega}^4 + l_8 \bar{\omega}^3 + l_9 \bar{\omega}^2 + l_{10} \bar{\omega} + l_{11}\right) I_n(h\bar{k}_1)}{l_{12} I_n(h\bar{k}_1) + (-\bar{\omega} + l_{13}) I_n'(h\bar{k}_1)} = 0 \tag{20}$$

where

$$\bar{k}_1 = \bar{k} \sqrt{1 - \frac{l_{14}}{(-\bar{\omega} + l_{13})}}$$

The coefficients $\{l_j\}$ depend on wave number $\bar{k}$, n, flow conditions, fluid properties, and geometric parameter and are available in Ref. 20. Note that as swirl is absent, the preceding dispersion equation reduces to a fourth-order polynomial equation and can be solved analytically. However, when air swirl is present, the dispersion equation does not have a closed form solution and, hence, is solved numerically by the secant method, which requires two initial guess values. A solution is considered convergent when the value of the left-hand side of Eq. (20) is smaller than 10^{-6}. Results from inviscid cases were taken as guess values for the viscous cases. Also, when air swirl is present, guess values were taken from the corresponding nonswirling cases. The nondimensional parameter space consists of the axial Weber numbers We_i, We_o, and We_l; the swirl Weber numbers We_{si} and We_{so}; the Reynolds number Re; the gas/liquid density ratios $\bar{\rho}_i$ and $\bar{\rho}_o$; the ratio of inner and outer radii h; the axial wave number $\bar{k}$; and the azimuthal wave number n. Given the flow conditions, fluid properties, and liquid film geometry, we solve for the root with the largest imaginary part, which represents the growth rate of a disturbance. The effects of liquid viscosity (Reynolds number), axial velocity (axial Weber number), and swirl velocity (swirl Weber number) on the growth rates of both the axisymmetric and helical modes are investigated.

III. Results and Discussion

Because the axial velocity of the liquid sheet is much lower than that of either the inner or outer airstream in a practical airblast atomizer, the value of axial Weber number based on liquid velocity, We_l, is kept as a constant of 37. This value corresponds to a liquid velocity of 1 m/s, a density of 1000 kg/m^3, a surface tension of 0.073 kg/s^2, an inner radius R_a of 2.5 mm, and a film thickness of 0.2 mm. Hence, by varying the axial Weber number of the airstreams, we can understand the effect of the relative axial velocity between the gas and liquid phases on the instability of the liquid sheet. Also, in this study, air/liquid density ratio and ratio of inner/outer radii are taken as 0.00129 and 0.90, respectively. Note that values of flow parameters considered here are within the range of practical operating conditions. For example, based on an airblast atomizer with an orifice diameter of 5 mm and liquid surface tension of 0.073 kg/s^2, a 30-m/s air speed corresponds to an air Weber number of approximately 40. Therefore, we have presented results with air Weber number up to 40. Effects of flow parameters on growth rates of the axisymmetric and helical modes are compared and examined in detail under both nonswirling and swirling flow conditions. Effect of liquid viscosity on the growth of various modes has also been investigated.

A. Without Air Swirl

Effect of axial velocity of the two airstreams on the growth rate of the axisymmetric and helical modes is shown in Fig. 3, a dispersion diagram showing the variation of growth rate with wave number. With both inner and outer air moving axially, the liquid sheet becomes unstable to a finite range of wave numbers with positive growth rates. Indeed, there exists a dominant wave number with the highest growth rate. This has been observed in previous experiments and can be explained as follows. The instability mechanism can be thought of as a frequency-selective amplifier. The mean flow is its energy supply, and its gain and frequency characteristics depend on flow parameters, fluid properties, and boundary conditions. Figure 3a is the dispersion diagram, when axial relative velocity is very low. Note that the axisymmetric mode ($n = 0$) has much higher growth rates than helical modes and, thus, dominates the competition of disturbance growth. As the axial velocity increases, as shown in Figs. 3b and 3c, both the maximum growth rate and the range of unstable wave numbers increase. Meanwhile, the corresponding most unstable wave number shifts to a higher value. As demonstrated in a recent study,[15] the higher the maximum growth rate is, the shorter the breakup length is. That study also revealed that the larger the most unstable wave number is, the smaller the size of droplets formed is. Therefore, increasing the relative axial velocity between the airstream and the liquid sheet significantly enhances the instability of the liquid sheet and, thus, improves the

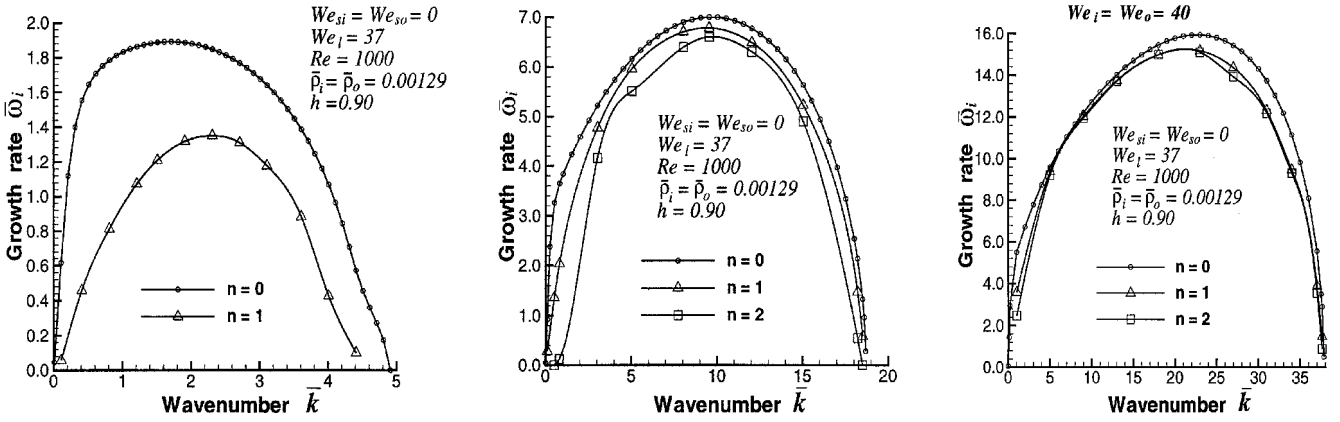

a) $We_i = We_o = 5$ b) $We_i = We_o = 20$ c) $We_i = We_o = 40$

Fig. 3 Dispersion diagrams corresponding to three different axial Weber numbers.

performance of airblast atomizers. A number of experimental measurements reported in literature[17–19] confirm this behavior.

We also note that, as the relative gas axial velocity increases, the importance of the first two helical modes becomes comparable to that of the axisymmetric mode. This implies a noncircular appearance of the annular liquid sheet at the breakup location under high-speed nonswirling flow conditions. However, as long as air swirl is absent, the axisymmetric mode remains to be the dominant mode and controls the breakup of the liquid sheet. Therefore, it is important to investigate how the maximum growth rate and the most unstable wave number of the axisymmetric mode are affected by the axial Weber number.

The maximum growth rate and the most unstable wave number are plotted against the axial Weber number in Figs. 4a and 4b, respectively. The results presented correspond to three different flow conditions, that is, with only inner air moving, with only outer air moving, and with both inner and outer air moving. It is found that the relationship between the maximum growth rate and the axial Weber number is essentially nonlinear when axial Weber number is smaller than 10, as shown in Fig. 4a. More important, we found that a combination of the inner and outer airflows leads to higher growth rates than only the inner air or only the outer air. Also the growth rate caused by the inner air is higher than that caused by the outer air. Figure 4b shows that the most unstable wave number has the largest value when both the inner and the outer airflows are present. Hence, a combination of the inner and the outer air is more effective in enhancing the instability of the liquid sheet than a single airflow and, thus, leads to a shorter breakup length.

The effect of liquid viscosity on the growth rates of the first three unstable modes is presented in Fig. 5. It is evident that both the maximum growth rate and the most unstable wave number decrease as liquid viscosity increases (or Reynolds number decreases). This indicates that liquid viscosity has a stabilizing effect on the liquid sheet. In addition to the damping effect, liquid viscosity also shifts the dispersion diagram toward long wavelength (or small wave number). This shifting effect on a higher mode is stronger than on a lower mode, leading to an overlap of dispersion diagrams corresponding to different Reynolds numbers in the small wave number region as shown in Figs. 5b and 5c. However, the axisymmetric mode has the highest growth rate among all unstable modes.

To better illustrate how liquid viscosity affects the breakup of the liquid sheet, the maximum growth rate and the most unstable wave number of the axisymmetric mode are plotted against Reynolds number in Figs. 6a and 6b, respectively. As the Reynolds number increases (or liquid viscosity decreases), both the maximum growth rate and the most unstable wave number increase dramatically at first and then gradually approach the values corresponding to the inviscid case. This trend reveals the damping effect of liquid viscosity on the growth of unstable waves. It also demonstrates that our previous inviscid model[16] can be recovered from the present theory in the limit of large Reynolds number.

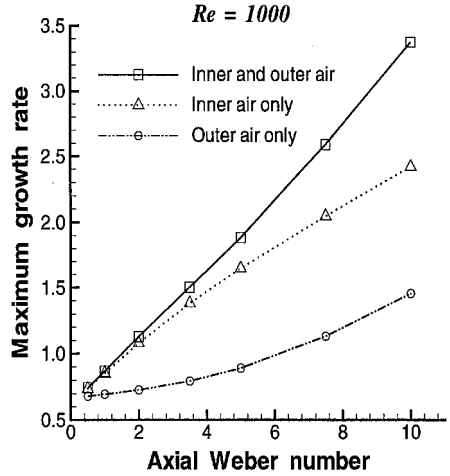

Fig. 4a Variation of the maximum growth rate with axial Weber number.

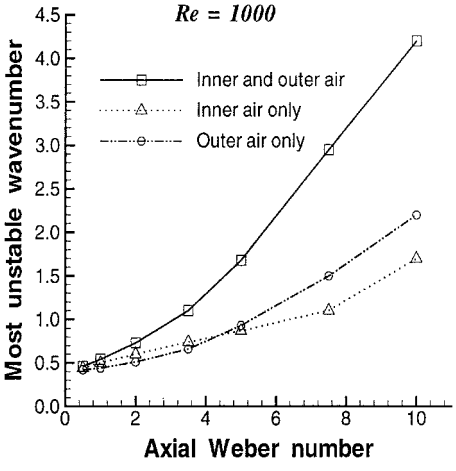

Fig. 4b Variation of the most unstable wave number with axial Weber number.

B. With Air Swirl

1. Inner Air Swirl Effect

To stabilize the flame and enhance air/fuel mixing inside a gas turbine combustor, swirl is imparted to the inner and outer airstreams as well as to the liquid fuel. The effect of liquid swirl on the instability of the liquid sheet emanating from a pressure-swirl atomizer has been considered in a recent paper.[15] Therefore, the present paper is mainly focused on the effects of the air swirl on the growth rates of

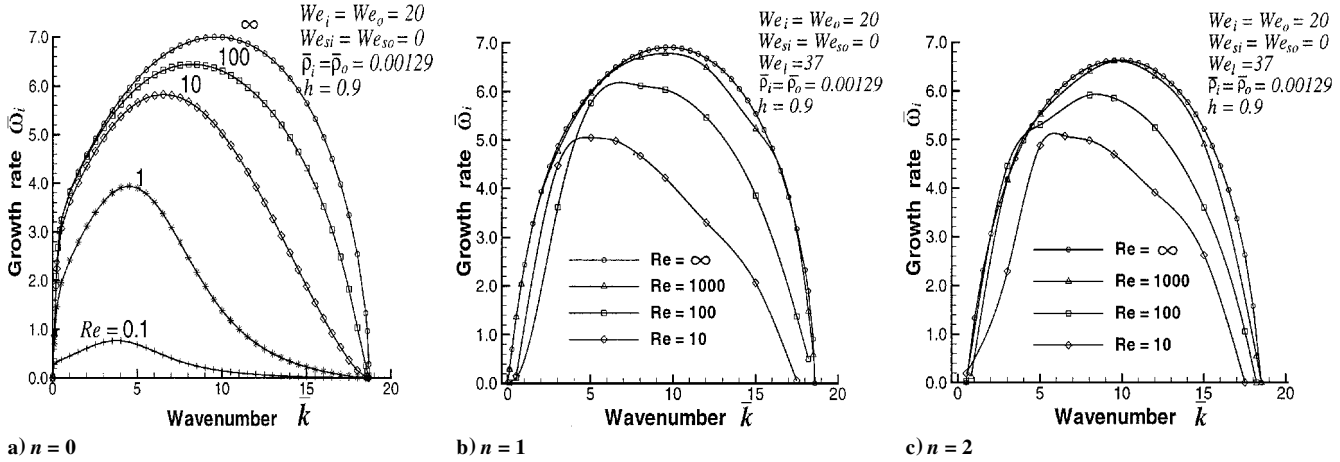

Fig. 5 Effect of liquid viscosity on growth rates of the first three modes.

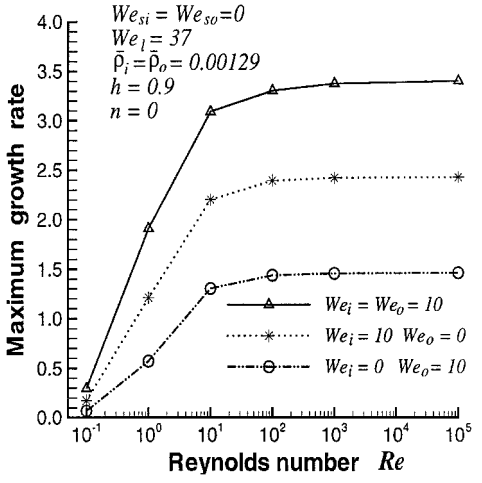

Fig. 6a Variation of the maximum growth rate with Reynolds number.

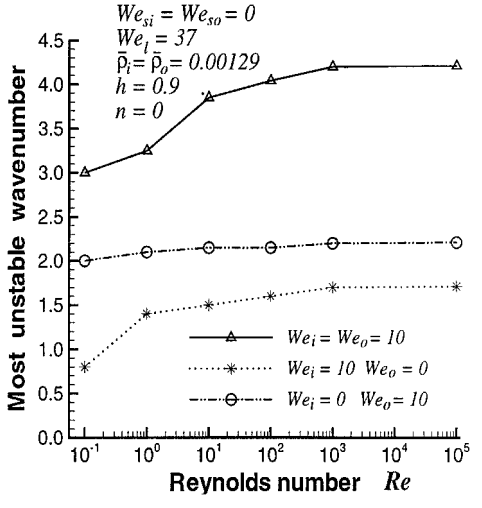

Fig. 6b Variation of the most unstable wave number with Reynolds number.

various unstable modes in the presence of liquid viscosity. Effectiveness of the inner and outer air swirl in promoting the breakup of the liquid sheet has also been investigated.

Figure 7 is the dispersion diagram for the flow condition where swirl is added only to the inner air. We find that features of the dispersion diagram have changed significantly from those corresponding to nonswirling flow condition. For nonswirling cases, the axisymmetric mode has the highest growth rate and dominates the breakup of the liquid sheet. However, when swirl is imparted to the inner air, both the maximum growth rate and the most unstable wave number of a higher helical mode are higher than those corresponding to the axisymmetric mode. As a result, the dominant mode is switched from the axisymmetric mode to a helical mode. This explains why the inner air swirl improves the performance of airblast atomizer, as reported in previous theoretical and experimental studies.[16,19] However, note that the instability theory only computes the growth rates of unstable waves and can not predict how liquid breakup takes place. A physical breakup model is needed to predict the breakup length and the resultant droplet sizes as described in a recent paper.[15]

As air swirl strength is increased, the growth rate of a higher helical mode is increased more significantly than the axisymmetric mode, making the higher helical mode more dominating. This implies that swirl is more effective in enhancing the helical mode than the axisymmetric mode. This behavior is similar to air swirl effect on inviscid annular liquid sheets.[16] Moreover, a local maximum and a minimum appear in the region of small wave numbers for the axisymmetric mode. However, as liquid viscosity is further increased, the local maximum and minimum are smeared out and eventually disappear. In summary, the inner air swirl has a destabilizing effect on the instability of the liquid sheet and improves the airblast atomization.

2. *Outer Air Swirl Effect*

The dispersion diagram is shown in Fig. 8 when only outer air is swirling. It is found that the outer air swirl also switches the dominant mode from the axisymmetric mode to a helical mode. Furthermore, the outer air swirl increases the growth rate of a higher helical mode more significantly than the axisymmetric mode. This demonstrates that the outer air swirl also enhances the instability of the liquid sheet and improves the performance of airblast atomizer. However, with an increase in the outer air swirl strength, the growth of the axisymmetric mode is decreased. Therefore, the outer air swirl inhibits the growth of the axisymmetric mode while it promotes the helical modes significantly.

3. *Both Air Swirl Effect*

Features of the dispersion diagram for the case where both inner and outer air swirl are present are shown in Fig. 9. Because of the contribution from both swirling airstreams, growth rate of the second helical mode is much higher than that of either the axisymmetric or the first helical mode. This demonstrates that a combination of the inner and outer air swirl is much more effective in promoting the instability of the liquid sheet than a single stream with air swirl and will lead to significant improvement of airblast atomization. Furthermore, it was revealed by the experimental study[19] that a combination of corotating inner airstream and counterrotating outer airstream with respect to the rotational direction of the liquid sheet produces the finest spray. However, for the axisymmetric mode, the combined air swirl effect is to reduce the growth rate in the small

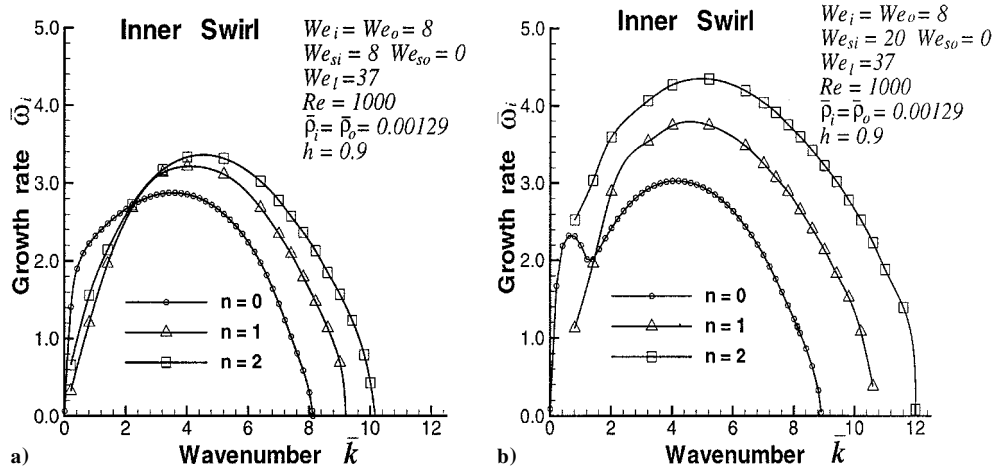

Fig. 7 Dispersion diagrams with only inner air swirl at a) $We_{si} = 8$ and b) $We_{si} = 20$.

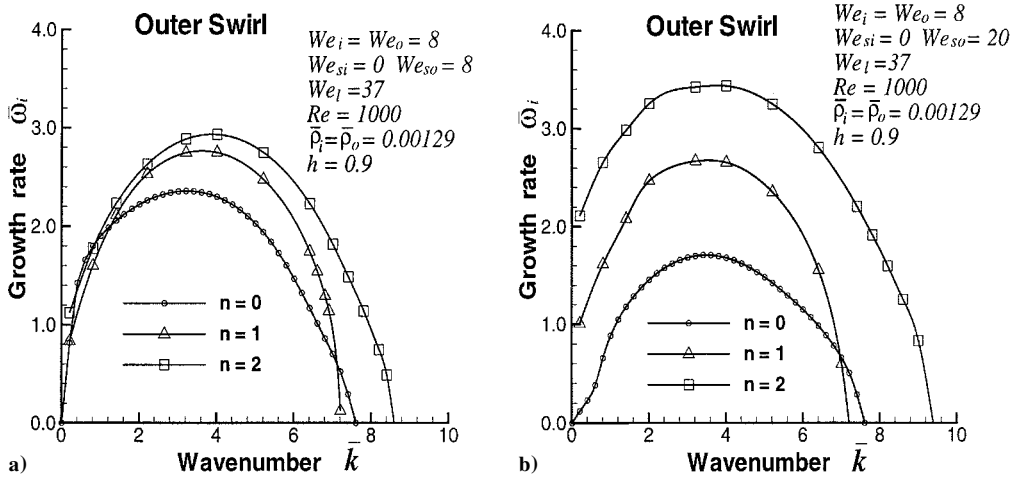

Fig. 8 Dispersion diagrams with only outer air swirl at a) $We_{so} = 8$ and b) $We_{so} = 20$.

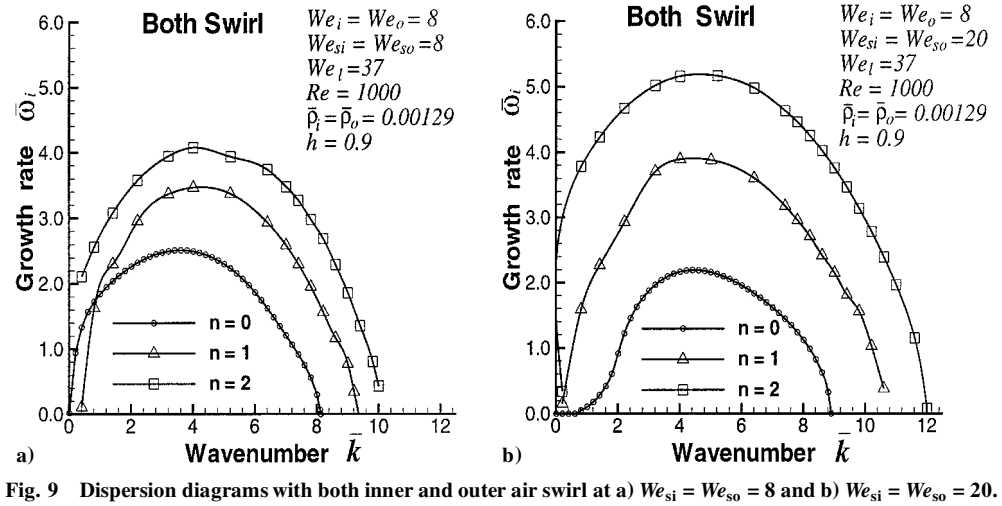

Fig. 9 Dispersion diagrams with both inner and outer air swirl at a) $We_{si} = We_{so} = 8$ and b) $We_{si} = We_{so} = 20$.

wave number region while increasing the growth rate in the large wave number region. This combined effect is due to the competition between the inner and outer air swirl in enhancing or inhibiting the growth of that mode.

4. Comparison of Air Swirl Effectiveness

To elucidate the effectiveness of air swirl in promoting the instability of the liquid sheet, growth rates of the first three modes are compared in Fig. 10 under the four different flow conditions, that is, no swirl, only inner air swirl, only outer air swirl, and both inner and outer air swirl. As shown in Fig. 10a, for the axisymmetric mode, the inner air swirl increases the growth rate in the large wave number region, whereas the outer air swirl reduces it within the unstable range. The net effect of the combined air swirl on the axisymmetric mode is to inhibit it in the small wave number region while promotes it in the large wave number region. For the helical modes, however, the combined air swirl is more effective than a single air swirl in enhancing their instability, as shown in Figs. 10b and 10c. The inner

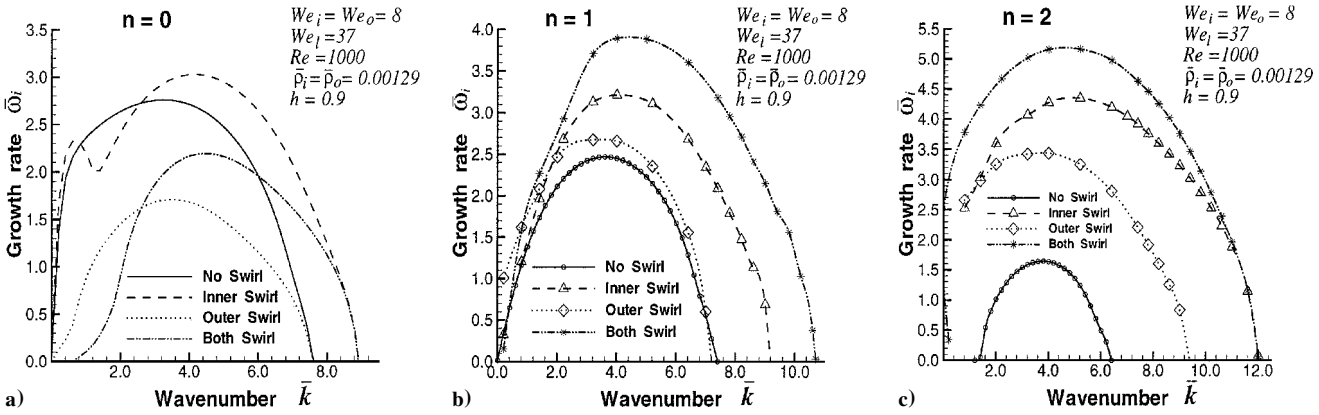

Fig. 10 Comparison of swirl effectiveness for the first three modes.

air swirl is more effective than the outer air swirl. In summary, to improve the airblast atomization process significantly, swirl should be imparted to both the inner and outer airstreams.

IV. Conclusions

An advanced stability model has been developed to predict the instability of an annular liquid sheet downstream of an airblast atomizer. Features of the model include three-dimensional disturbances, liquid viscosity, inner and outer air swirl, and annular liquid sheet with finite thickness. The air swirl profile considered in the model is a combination of solid body rotation and free vortex type. Effects of flow conditions and liquid viscosity on the growth of the first three modes are investigated. It is observed that the relative axial velocity between the liquid and the gas phases promotes the breakup of the liquid sheet by increasing the maximum growth rate and the most unstable wave number. At low velocities, a combination of the inner and outer airstreams is more effective in disintegrating the liquid sheet than only the inner or only the outer airstream. Without air swirl, the axisymmetric mode is the dominant mode in the breakup process of the liquid sheet. Liquid viscosity not only reduces the growth rates of unstable modes, but also shifts the dispersion diagram toward long waves. The shifting effect of liquid viscosity on a higher helical mode is stronger than on a lower helical mode. As Reynolds number increases, both the maximum growth rate and the most unstable wave number increase dramatically at first and then gradually approach values corresponding to the inviscid case. Air swirl not only increases the maximum growth rate and the most unstable wave number, but also switches the dominant mode from the axisymmetric mode to a helical mode. The enhancement of a helical mode is more significant than the axisymmetric mode. A combination of the inner and outer air swirl is more effective than a single air swirl in enhancing the instability of the liquid sheet and in improving airblast atomization, whereas the inner air swirl is more effective than the outer air swirl.

Acknowledgments

Sponsorship of this work by Parker Hannifin Corporation and NASA John H. Glenn Research Center at Lewis Field under Grant NAG3-1987 is greatly appreciated.

References

[1]Lefebvre, A. H., "Airblast Atomization," *Progress in Energy and Combustion Science*, Vol. 6, No. 3, 1980, pp. 233–261.

[2]Rizk, N. K., Chin, J. S., and Razdan, M. K., "Modeling of Gas Turbine Fuel Nozzle Spray," *Journal of Engineering for Gas Turbines and Power*, Vol. 119, No. 1, 1997, pp. 34–44.

[3]Squire, H. B., "Investigation of the Instability of a Moving Liquid Film," *British Journal of Applied Physics*, Vol. 4, June 1953, pp. 167–169.

[4]Hagerty, W. W., and Shea, J. F., "A Study of the Stability of Plane Fluid Sheets," *Journal of Applied Mechanics*, Vol. 22, No. 4, 1955, pp. 509–514.

[5]Clark, C. J., and Dombrowski, N., "Aerodynamic Instability and Disintegration of Inviscid Liquid Sheets," *Proceedings of the Royal Society of London, Series A: Mathematical and Physical Sciences*, Vol. 329, No. 1579, pp. 467–478.

[6]Dombrowski, N., and Johns, W. R., "The Aerodynamic Instability and Disintegration of Viscous Liquid Sheets," *Chemical Engineering Science*, Vol. 18, No. 3, 1963, pp. 203–214.

[7]Li, X., and Tankin R. S., "On the Temporal Instability of a Two-Dimensional Viscous Liquid Sheet," *Journal of Fluid Mechanics*, Vol. 226, May 1991, pp. 425–443.

[8]Mansour, A., and Chigier, N., "Dynamic Behavior of Liquid Sheets," *Physics of Fluids A*, Vol. 3, No. 12, 1991, pp. 2971–2980.

[9]Kamler, R., "Modeling Dynamic Behavior of Liquid Sheets," M.S. Thesis, Dept. of Aerospace Engineering and Engineering Mechanics, Univ. of Cincinnati, Cincinnati, OH, 1998.

[10]Crapper, G. D., Dombrowski, N., and Pyott, G. A. D., "Kevin–Helmholtz Wave Growth on Cylindrical Sheets," *Journal of Fluid Mechanics*, Vol. 68, No. 3, April 1975, pp. 497–502.

[11]Meyer J., and Weihs, D., "Capillary Instability of an Annular Liquid Jet," *Journal of Fluid Mechanics*, Vol. 179, No. 6, June 1987, pp. 531–545.

[12]Lee, J. G., and Chen, L.-D., "Linear Stability Analysis of Gas–Liquid Interface," *AIAA Journal*, Vol. 29, No. 10, 1991, pp. 1589–1595.

[13]Shen, J., and Li, X., "Instability of an Annular Viscous Liquid Jet," *ACTA Mechanica*, Vol. 114, Nos. 1–4, 1996, pp. 167–183.

[14]Panchagnula, M. V., Sojka, P. E., and Santangelo, P. J., "On the Three-Dimensional Instability of a Swirling, Annular, Inviscid Liquid Sheet Subject to Unequal Gas Velocities," *Physics of Fluids*, Vol. 8, No. 12, 1996, pp. 3300–3312.

[15]Liao, Y., Sakman, A. T., Jeng, S. M., Jog, M. A., and Benjamin, M. A., "A Comprehensive Model to Predict Simplex Atomizer Performance," *Journal of Engineering for Gas Turbines and Power*, Vol. 121, No. 2, 1999, pp. 285–294.

[16]Liao, Y., Jeng, S. M., Jog, M. A., and Benjamin, M. A., "Instability of an Annular Liquid Sheet Under Swirling Air Streams," *AIAA Journal*, Vol. 38, No. 3, 2000, pp. 453–460.

[17]Lavergne, G., Trichet, P., Hebrard, P., and Biscos, Y., "Liquid Sheet Disintegration and Atomization Process on a Simplified Airblast Atomizer," *Journal of Engineering for Gas Turbines and Power*, Vol. 115, No. 3, 1993, pp. 461–466.

[18]Carvalho, I. S., and Heitor, M. V., "The Break-up of a Annular Liquid Sheet Downstream of an Airblast Prefilming Atomizer," *Proceedings of the 10th Symposium on Turbulent Shear Flows*, Vol. 3, Pennsylvania State Univ., Univ. Park, PA, pp. P3-97–P3-102.

[19]Chin, J. S., Rizk, N. K., and Razdan, M. K., "Effect of Inner and Outer Air Flow Characteristics on High Liquid Pressure Prefilming Airblast Atomization," *Proceedings of the 13th International Symposium on Airbreathing Engines*, 1997, pp. 521–527.

[20]Liao, Y., "Instability and Breakup of Liquid Sheets and Liquid Jets," Ph.D. Dissertation, Dept. of Aerospace Engineering and Engineering Mechanics, Univ. of Cincinnati, Cincinnati, OH, Jan. 1999.